Study of Archean chromites from Mysore district, Western Dharwar Craton - compositional variations, thermometry and possible parental magmas

Thesis submitted towards the partial fulfillment of the M.Sc. final examination in Applied Geology of Jadavpur University, 2019

Under the guidance of
Professor Sisir K. Mondal

By
Priyanjan Datta
MGEO194016
Department of Geological Sciences
Jadavpur University

To my parents, who tried their best

যাদবপুর বিশ্ববিদ্যালয়
কলকাতা-৭০০ ০৩২, ভারত

JADAVPUR UNIVERSITY
KOLKATA-700 032,INDIA

FACULTY OF SCIENCE : DEPARTMENT OF GEOLOGICAL SCIENCES

Certified that **Priyanjan Datta**, Class Roll No. **001720402016**, a student of the M.Sc. Final Year, Department of Geological Sciences, has conducted research work under me for his dissertation thesis on **'Study of Archean chromites from Mysore district, Western Dharwar Craton - compositional variations, thermometry and possible parental magmas'**. He has carried out his dissertation under my supervision for the partial fulfillment of the M.Sc. Final Examination (Applied Geology), 2019. This dissertation work is based on hand specimen studies, sample preparation and detailed microscopy (both transmitted and reflected light), EPMA of minerals along with extensive data handling, graphical plots and interpretation of the acquired data. **Priyanjan Datta** has successfully completed his dissertation with sincerity and dedication. The outcome of this research is worth publishing in an international or national journal as well as presentable to the conference or symposium.

Sisir Kanti Mondal
30/5/19

Sisir Kanti Mondal
Supervisor

Dr. Sisir Kanti Mondal
Professor
Department of Geological Sciences
Jadavpur University
Kolkata - 700032

30/05/2019

Head
Department of Geological Sciences
Jadavpur University
Kolkata-700032

দূরভাষ : ২৪১৪-৬৬৬৬/প্রসারণ : ২২৬৮

Website :www.jadavpur.edu
E-mail : hod_geological@jdvu.ac.in

Phone: 2414-6666 Extn. 2268

Acknowledgement

I would like to take this opportunity to thank Prof. Sisir K. Mondal for giving me a platform to express my ideas freely and training me up efficiently for this dissertation work. His words of expertise will always be helpful in my future adventures. I would also like to acknowledge DST-PURSE-Phase-II, Jadavpur University and CEFIPRA-Indo-French International Collaborative Research Project 6007-1 to Prof. Sisir K. Mondal for analytical support in my work.

Contents

Abstract

1. Introduction
2. Regional Geology
3. Geology of the Archean Ultramafic-mafic belt
4. Methodology
5. Description of the rocks
6. Petrography
7. Mineral chemistry

7.1. Silicates

7.2. Chromite

8. Discussion

8.1. Compositional variations

8.2. Olivine-chromite thermometry

8.3. Implications

9. Conclusion

References

Abstract

The Sargur greenstone belts occur as enclaves of metavolcanics, metasediments, basic granulites and serpentinized ultramafics embedded in a granodioritic continental crust. Talur, Sindhuvalli and Doddakanya is in this high-grade terrain. In Talur, chromite deposits are associated with magnesite deposits. In Sindhuvalli and Doddakanya, there are chromite deposits. Detailed studies reveal intense compositional variability of the chromite grains in silicate-rich chromitite (≈50% modal chromite) and serpentinite (≈2% modal chromite) throughout the entire ultramafic sequence. However, the primary composition of chromite is preserved in the massive chromitites (≈60-75% modal chromite) from Talur and Sindhuvalli deposits in the Sargur schist belt. In Talur, the chromites in massive chromitite is characterized by relatively lower Mg# (0.28-0.39) compared to chromites from massive chromitite in Sindhuvalli (0.63-0.69). This might signify that the parental melt associated with chromites in Talur was more fractionated compared to the melt associated with chromites from massive chromitite in Sindhuvalli. The primary Fo content of olivine in dunites from Talur (Fo_{91-92}) showed lower values compared to olivine in dunites from Doddakanya (Fo_{92-93}). This signifies that the parental melt in Talur was also more evolved compared to the parent melt in Doddakanya. The accessory chromites in dunite from Talur show higher Cr#, Fe^{3+}#, TiO_2 and MnO compared to other samples. This is due to sub-solidus re-equilibration associated with alteration and metamorphism. From olivine-chromite thermometry, the re-equilibrated temperatures obtained from olivine-chromite pairs in dunite from Doddakanya is 674-884 °C and olivine-chromite pairs in net-textured chromitite in Sindhuvalli is 708-750 °C. This temperature corresponds to the stability field of amphibolite facies metamorphism. In Talur-dunite, the chromite-olivine pairs have re-equilibrated to temperature of 477-537 °C which coincides with the stability field of talc and

magnesite. The calculated Al_2O_3, FeO/MgO ratio and TiO_2 content of the parental melt shows close resemblance with the komatiitic parent melt of chromites in the Nuggihalli greenstone belt, Western Dhawar craton. The compositions of chromite from massive chromitite in Cr#-Mg# plot as well as in the Fe^{3+} -Cr-Al ternary plot the samples from Sargur greenstone belt fall in the field of chromites from komatiites metamorphosed to greenschist and amphibolite facies.

1. Introduction

Chromite chemistry is regarded as an important indicator of petrogenesis of ultramafic-mafic igneous complexes (Mondal et al., 2006). The chemistry of chromite in the ultramafic-mafic complexes is generally affected during subsolidus cooling such as due to interactions with the co-existing melt and minerals and variable degrees of alteration and metamorphism (Mondal et al., 2006). As a result, original geochemical signatures are either blurred or nearly obliterated and one has to carefully look for whatever relic primary features still exist to unravel the petrogenetic history of the igneous complex.

Archean greenstone belts represent the site of continental crustal growth in the early Earth. The greenstone belts are composed of interlayered volcano-sedimentary rocks that are surrounded by the tonalite-trondhjemite-granodiorite (TTG) gneisses. Sill-like layered bodies of plutonic ultramafic and mafic rocks comprise an important component of Archean greenstone belts, as for example in the Shurugwi greenstone belt (Zimbabwe craton; Stowe, 1987), Sukinda-Nuasahi-Jojohatu complexes in the Iron Ore Group (IOG) greenstone belts (Singhbhum craton, eastern India; Mondal et al., 2006), Nuggihalli-Holenarsipur-Krishnarajpet-Banasandra-Kalyadi greenstone belts (Western Dharwar craton, southern India; Mukherjee et al., 2010), Jamestown igneous complex in Barberton greenstone belt (Kaapvaal craton, South Africa; DeWit et al., 1987), Bird River sill within the Bird River greenstone belt (Superior craton, Canada; Ohnenstetter et al., 1986; Mungall and Staff, 2008), and the Obanga greenstone belt (Superior craton, Canada; Tomlinson et al., 2002). These ultramafic-mafic bodies are genetically related to high-Mg magmas such as komatiite, boninite or high-Mg siliceous basalt (Mondal et al., 2001, 2006, 2007; Prendergast, 2008; Rollinson, 1997).

Similar type of sill-like layered ultramafic bodies with chromitite seams are present within early Archean Sargur Group supracrustal rocks at the southern part of the Western Dharwar craton (**Fig. 1**). Samples of the host ultramafic rocks and the chromitites were collected from three mining areas namely Talur, Dodakanya and Sindhuvalli belonging to the Mysore district, where the ore bodies are surrounded by serpentinized dunite and associated with magnesite. The chromitite bearing plutonic ultramafic bodies are present within the Sargur greenstone belt (or Sargur schist belt) comprising of metasedimentary and metavolcanics rocks. Although the occurrences of chromite deposits are known for the last 4-5 decades, however, detailed petrographic, mineralogical and petrological study of these ultramafic rocks and the chromitites are not undertaken so far. In this dissertation research work I have conducted detailed study of these rocks including the chromitites to determine the compositional variability of chromites and the co-existing minerals in different rocks from the above three locations. It is essential, as these rocks are part of a deformed, altered and metamorphosed Archean greenstone sequence, where compositional variability is expected within minerals including chromite. The main goal of this study is to characterize the chromite from petrographic and mineralogical studies in order to understand the parental melt character, the genesis, sub-solidus history and other secondary processes that may have acted upon the chromite grains, thereby inducing variability in their compositions. In addition, thermometric calculations have been conducted using olivine-spinel geothermometer to understand the extend of re-equilibration of co-existing olivine-chromite pairs in different rocks such as dunite, net-textured chromitite, schlieren banded chromitite and massive chromitite as the whole assemblages bear the evidences of alteration and metamorphism.

2. Geological background

A 500 km long, N-S trending intrusive body of Closepet Granite (2.5 Ga; Taylor et al., 1988) has sub-divided the Dharwar craton into a western and an eastern component. The Western Dharwar craton comprises older Archean supracrustal rocks that constitute the Sargur Group (Swami Nath and Ramakrishnan, 1981). The Sargur Group consists of sediments and igneous rocks that were metamorphosed to greenschist and amphibolite facies. The meta-igneous lithologies occur as both intrusive and volcanic ultramafic-mafic rocks with a compositional range from komatiite to komatiitic basalts and tholeiites (Ramakrishnan et al., 1994). The ultramafic-mafic rock bodies occur as linear belts, and are associated with clastic sediments (mainly quartzites) and banded iron formations, as found in the greenstone belts of Nuggihalli, Holenarsipur, Krishnarajpet, and Nagamangala. Rocks of the Sargur Group are unconformably overlain (Swami Nath and Ramakrishnan, 1981) by the younger supracrustals of the Dharwar Supergroup (younger greenstone belts ≈2.9-2.6 Ga; Taylor et al., 1984). The Dharwar Supergroup overlies the tonalite-trondhjemite-granodiorite (TTG) suite that acts as their basement, and is later intruded by the Closepet Granite at about 2.5 Ga.

The Archean greenstone belts, comprising the Sargur Group of rocks, commonly occur as long linear belts (≈length 60-100 km; width ≈1-3 km) with a NNW-SSE trend. Among these the Nuggihalli greenstone belt consists of several en-echelon, lenticular, dismembered, sill-like ultramafic-mafic bodies that are well exposed in the Tagdur mining area belonging to the Hassan district (Mukherjee et al., 2010; 2012; 2014; 2015). The sill-like bodies are composed of layers of dunite (now serpentinite), peridotite (now tremolite–chlorite–actinolite schist), pyroxenite and gabbro. The sequence commences with a serpentinite and tremolite–chlorite–actinolite schist unit that hosts the chromitite ore bodies (≈ 50–500 m

length; width ≈15 m). The chromitites appear as sigmoidal, lenticular, pod-shaped, and folded bodies (≈0.5 m length; width ≈0.3 m), with a nearly vertical dip (75°- 80°) and a range in strike from NW-SE to N-S with dip towards the east; at places, they also have an E–W trend with dip towards the north (Mukherjee et al., 2010). The serpentinite and peridotite are overlain by a pyroxenite unit, which is subsequently followed by a gabbro unit. The gabbro shows layering, and contains two conformable bands of titaniferous–vanadiferous magnetite at the base and top of the unit. The upper magnetite band has a N–S trend (width ≈1 m; Radhakrishnan et al., 1973), whereas the lower band (width ≈2 m) trends in the NNW-SSE direction; both dip towards the east. The gabbro is overlain by an upper ultramafic unit of chromitite bearing serpentinite. The chromitites (N–S trend, dipping west) in this unit are elongated, lenticular (length ≈ 100 m; width ≈ 15 m), and are more altered with a higher mode of carbonate (mainly magnesite). The upper ultramafic unit is overlain by the schists that are variably altered, and possess a strong deformational fabric which imparts a lens-shaped geometry to the rocks (Mukherjee et al., 2012). A lens-shaped E–W trending anorthosite unit (width ≈130 m) is observed in the Jambur mine, where it is interlayered with serpentinite. Overall, the rocks in the Nuggihalli greenstone belt are deformed and altered, with the deformation and alteration being linked to later metamorphism and secondary low temperature hydrothermal processes during serpentinization (Mukherjee et al., 2010).

3. Geology of the chromite deposits of Sargur greenstone belt, Mysore district

The poly-metamorphosed Sargur greenstone belt consists of a number of N-S to NNE-SSW trending enclaves of metavolcanic-metasedimentary rocks, basic granulites, amphibolites and serpentinised ultramafic bodies within the gneissic country rock of

granodiorite composition (Venkatarama et al., 1982). The enclaves vary in thickness from a few metres to up to 2 km. Numerous granitic rocks, felsic and mafic sills and dykes intrude and cut-across the older rocks. Several chromite deposits occur near Sinduvalli, Talur and Udbur areas of Mysore district (Venkatarama et al., 1982). Small occurrences have been reported from Nachenahalli, Woddarapalya, Gurur, Doddakanya, Doddakatur, Uttanahalli, Marasettihalli, Solepura and Iyerahalli areas of Mysore district. Among the chromite deposits, the ore bodies in the Sinduvalli block, about 6 km west of Kadakola railway station is the largest. The Talur mining block is about 1 km west of Sinduvalli, which has been yielding 45 to 47 % Cr_2O_3 ore (Venkatarama et al., 1982).

***Geological features of the Sindhuvalli-Talur belt*:** The Sindhuvalli-Talur belt, a part of the high-grade Sargur schist belt, extends from River Kabini to the southern limits of Mysore city (**Fig. 1**) and has a general N-S trend. According to Venkatarama, the main lithological units in this belt are (i) Sargur Group supracrustals comprising of amphibolites, metapelites, semipelites, marbles and quartzites, (ii) biotite gneiss of granodiorite composition and its local modifications, (iii) basic granulites, (iv) chromite-bearing serpentinized ultramafic plutonic sequence and metagabbro, (v) late stage acid igneous rocks, and (vi) basic dykes.

(i) Sargur Group Supracrustal rocks - Among the metavolcanic rocks amphibolites occur as randomly oriented fragments within the biotite gneiss or as mafic components interleaved with the gneisses belonging to the TTG suite. Most of the amphibolites are massive and have a granoblastic texture with the mineral assemblage of hornblende + plagioclase + clinopyroxene + almandine. Metasedimentary rocks are preserved in the area as pelitic schists and gneisses with the characteristic mineral assemblage of cordierite, sillimanite, garnet, biotite and graphite; quartzites with biotite, garnet and corundum. These rocks occur as lenticular bands along the borders between the chromite-bearing ultramafic-mafic

complex and the gneissic country rock of the TTG suite. Banded magnetite quartzite, carbonates and fuchsite quartzite horizons have been reported from adjacent parts of the belt (Janardhan et al., 1978).

(ii) Biotite gneiss of TTG suite - Biotite gneiss, the predominant rock type of the area, is mostly granodioritic in composition (Venkatarama et al.; 1982). Locally, the gneiss is garnetiferous in areas with enrichment of mafic minerals. At places white quartzo-feldspathic bands with the minimum of mafic minerals run parallel to the general foliation of the gneiss which trends N10°E to N10°W with steep dips (75-85°) both to the east and west. Because of the complex tectono-metamorphic history of the area it is difficult to distinguish the relative ages of the various gneissic components.

(iii) Basic granulites - Interleaved with the biotite gneisses are hornblende, hypersthene and two pyroxene-bearing basic rocks with typical granulitic texture (Venkatarama et al., 1982). These occur as bands, varying in thickness from a few centimetres to up to 5 m width, and can be traced for 4-20 m along the strike.

(iv) Chromite-bearing ultramafic-mafic plutonic suite - Numerous dismembered bodies of serpentinised ultramafic rocks, varying in thickness from a few metres to up to 500 m, are exposed over a stretch of 25 km from east of Byathalli to the west of Talur. These bodies, which occur as intrusives into biotite gneiss, are believed to be connected to larger bodies below as per gravity data (Qureshy et al., 1970). The contacts between the ultramafic rocks and the enclosing gneisses are steep and mostly sharp. Field studies in the magnesite quarries in Dodkanya area reveal that the ultramafic complex comprises a cyclic sequence of serpentinised dunite, harzburgite and hornblende-bearing peridotite occasionally inter-banded with layers of hornblendite, pyroxenite and chromitite (Venkatarama et al., 1982). These layers are subhorizontal to moderately dipping (45°) both to the east and west.

Surface exposures in Dodkatur area show that pyroxenite and hornblendite merge into each other, forming intermediate hornblende-pyroxenite and pyroxene-hornblendite rocks. In the old workings, west of Sindhuvalli, chromitite bands comprising nearly 90% coarse, euhedral chromite grains pass on to overlying dunite, pyroxenite or hornblendite. Rarely, crude graded bedding and phase-layering are observed in the ultramafic rocks. At places sheets of metagabbro, metanorite and meta-anorthosite are seen to be intimately associated with the ultramafic sequence. These ultramafic rocks are most abundant and best preserved in the Dodkatur area.

(v) Late-stage acid igneous rocks - Homogeneous fine-grained to porphyritic granite bosses are widely distributed within the biotite gneisses. Aplite and pegmatite veins cut across all the earlier formations.

(vi) Basic dykes - These are mostly doleritic and noritic in composition and comprise olivine, plagioclase, diopside, augite, enstatite and hypersthene. The dykes trend N-S to N 30°W and transect the foliation of the biotite gneisses and the serpentinised ultramafic rocks.

4. Methodology

Systematic sampling has been conducted across three different mining districts in the Sargur greenstone belt. They are namely Talur chromite and magnesite mines, Sindhuvalli mines and the Doddakanya chromite and magnesite mines. In total 13 samples were collected out of which 5 samples were from the Talur mines, 3 samples were from the Sindhuvalli mines and 5 samples were from the Doddakanya mines. At first samples were cut into 3 slices and cleaned very well by soap water. Among these three slices one was kept for sample preparation, one for future use and one for preparing slide. The slice used for slide preparation was cut again in the shape of a slide and sent to laboratory for thin section

preparation. After thin section was prepared the slides were polished using ¼ sized diamond paste and lubricating oil for better view under microscope and image analyser by removing the pits. The samples were studied meticulously under petrographic microscope (both transmitted and reflected light) and the observations were documented. Specific samples covering the study areas were chosen for Electron Probe Micro-analysis (EPMA) using Cameca SX-100 equipped with four wavelength dispersive spectrometers (WDS) at IIT Kharagpur, West Bengal, India. This was operated at acceleration voltage of 15kV, beam current of 20nA and beam size of 1µm. The standards that were used are Na – albite, Mg – periclase, Si – orthoclase, Ca – CaO, Ti – rutile, Cr – Cr_2O_3, Ba – BaSO4, Al – corundum, Mn – rhodonite, Fe – hematite, V – pure V, Ni - pure Ni, Zn – ZnS. The compositions of chromite are recalculated to cation proportions using the Fe^{3+} calculation scheme of Droop (1987).

5. Description of the host rocks and chromitites

Talur chromite and magnesite mines - A total of five samples are studied from this mining area. Among these one sample is of a dunite that hosts the chromitites. Dunite is the adcumulate of olivine with minor accessory chromites (**Fig. 3 a.**). Disseminated chromite and sulfide grains are identified through hand lens. Secondary alterations in the form of serpentine and magnesite veins are present in the sample. Presence of magnesite is verified as effervescence is observed on putting concentrated HCL on the sample. Formation of talc is also observed in some areas of dunite. On the basis of the study four different types of chromitite ores are identified i.e. massive chromitite, net-textured chromitite, and schlieren banded chromitite (**Fig. 3 b, c, d**). All the samples are extensively altered. Olivine in chromitites can be hardly distinguished in hand specimen scale. Patches of magnesite are present in all the samples. Based on the modal proportions of the intercumulus silicates the

chromitites can be identified as massive chromitite, net-textured, and schlieren banded varieties (**Fig. 3 b, c, d**). Highly altered olivine grains are present in association with the chromite grains. Olivine grains are subrounded to subhedral and shows secondary alteration products like serpentine, magnesite and talc. Magnesites occur as patches in hand specimen scale (**Fig. 3 c, d**). Fresh unaltered variety of chromite are also sampled and studied from this area. It has a much higher specific gravity. The chromite grains are coarse and showed saccharoidal texture (**Fig. 3 b**). In the schlieren banded chromitites, grains in association with olivine growing along the boundaries of the chromite grains (**Fig. 3 c**).

Sindhuvalli chromite mines - A total of three samples are studied from this area. Net-textured chromitite and massive chromitite are the two main variety of ores which are observed and documented (**Fig. 4 a, b**). The net-textured chromitites are composed of primary chromite and altered olivine grains. Secondary alteration products like magnesite and serpentine are common. Minor patches of chlorite are also identified. On the other hand, the massive chromitites are spared of any alterations. It has a high specific gravity, with minimum amount of interstitial minerals. The grains showed saccharoidal nature under hand-lens (**Fig. 4 b**).

Doddakanya chromite and magnesite mines - A total of five samples are studied from this area. The general rock type is dunite that hosts the chromitites. The dunite samples have overall greenish tinge (**Fig. 5**). Dunite is composed of olivine grains and disseminated accessory chromite grains. Magnesites are also observed in the samples which occur as veins as well as in patches. Overall dunite has less specific gravity compared to the massive chromitites. Some of the magnesite veins seemed to have been incorporated through fracture networks which might attest the fact that the rock suffered deformations at a later stage.

6. Petrography

Talur chromite and magnesite mines

Dunite – The rock is extensively altered to serpentinite. However, primary cumulate textures of the protolith are preserved (**Fig. 6 c**). The rock is highly deformed and veined by magnesite. Chrysotile is the major constituent in serpentinite along with minor lizardite. Serpentinite exhibits interpenetrative, mesh and pseudomorph textures. Disseminated chromite grains occur uniformly throughout the sample. Sulfide micro-spherical grains are observed showing high reflectance and bright yellow colour in reflected light. Other secondary minerals include talc, chlorite and ferrian-chromite.

Net-textured chromitite – The sample is composed of subhedral to anhedral chromite grains in association with serpentine (10 vol %) and magnesite (25 vol%) (**Fig. 6 b**). Tremolite occurs as long-bladed prismatic grains which were elongated. Chrysotile is the major constituent in serpentinite along with minor lizardite. Chromite contains inclusions of primary silicate minerals that are spherical to euhedral in shape and are of orthopyroxene, olivine and clinopyroxene. The inclusion minerals are often altered to serpentine, chlorite and magnesite bearing assemblages. Chlorite usually occurs as veining material within the chromite as well as along the grain boundary. Magnesite occurs as micro-veins within the chromite and at places they transgress serpentines. The interstitial serpentines in the chromitite mostly show interpenetrative and interlocking textures.

Massive chromitite – The sample is composed almost entirely of subhedral to anhedral chromite grains (**Fig. 6 d**). Some relicts of silicate grains are present at the interstitial spaces of chromites. Larger chromite grains are polygonal to subrounded and show moderate to high reflectance. The grains are relatively fresh without any alterations of secondary

minerals (**Fig. 6 d**). Some grains are fractured which may be due to later deformation. There are no observable inclusions in the chromite grains. Grain size are unimodal.

Schlieren-banded chromitite – The sample showed olivine grains growing along the boundaries of the chromite grains (**Fig. 6 a**). The chromite grains were subhedral to anhedral in form. Secondary alterations in the form of magnesite micro-veins and serpentinite were observed in the sample (**Fig. 6 a**). Both fibrous chrysotile and flaky lizardite variety serpentine are observed. The magnesite and the serpentine veins have a medium angle cross-cutting relationship where magnesite veins cut the serpentine veins (**Fig. 6 a**). Talc is also present in the sample as minor phase and it showed 4^{th} order variegated interference colour.

Sindhuvalli chromite mines

Net-textured chromitite – The rock is heavily altered comprising of olivine and chromite as the major constituents. Olivine and chromite grains show cumulate texture (**Fig. 7 a**). Olivines are altered to serpentine minerals. The fibrous chrysotile serpentine predominates in the sample. Magnesite grains are observed growing in association with serpentine. Some chromite grains are replaced by serpentine but magnesite grains are unaffected. The grain size of the chromite grains is bimodal. Most of chromite grains are extensively fractured which signify later deformational episodes. Minor clinoenstatite grains showing low extinction angles were also observed.

Massive chromitite – The chromite grains are mostly anhedral in nature, showing bimodal grain sizes (**Fig. 7 b**). The grains exhibit both spotted as well as larger polygonal shapes. The grains are free from any secondary alterations. Larger chromite grains are fractured. Some chromite grains have primary silicate mineral inclusions which could not be identified under microscope.

Doddakanya chromite and magnesite mines

Dunite – Olivine grains show cumulate texture and is extensively altered to serpentine-group of minerals (**Fig. 8**). Fibrous chrysotile serpentine is the most common alteration phase. Prominent magnesite micro-veins are observed in the rock. It cuts the serpentine minerals wherever the two met (**Fig. 8**). Minor chlorite is also documented. Chromites occur as a disseminated phase throughout the sample. The chromite grains are fractured. Cross-fibered serpentine is noticed in minor quantities in a narrow zone of the magnesite mine (**Fig. 8**). The development of mesh-textured serpentine was initiated along the grain boundaries of olivine and fractures in it. This mesh textured serpentinite contains relict of olivine grains (**Fig. 8**). Vein serpentine, which constitutes a minor phase, is confined to microfractures. It is essentially massive and is composed of lizardite. Vein serpentine often extends into mesh-textured serpentine.

In association with olivine and serpentine, primary pyroxene identified as clinoenstatite is also identified in the assemblage (**Fig**. **8**). The grains are subhedral and have a prismatic elongated nature. Two sets of prominent cleavages at right angles are seen almost in every grain.

A detailed description of the studied rock types with their locations and modal abundances are listed in **Table 1.**

7. Mineral chemistry

Olivine - The olivine grains from the 3 study areas are highly magnesian in nature (**Fig. 9**). The olivine from the net-textured chromitite in the Sindhuvalli region shows highest Mg-values (Fo_{95}) with a general range in between Fo_{94} and Fo_{96}. The olivine grains from the dunite in Talur mines show Mg-values in the range of $Fo_{91\text{-}92}$ **(Fig. 9)**. For Doddakanya area,

Mg-values are more or less uniform in all the samples (Fo_{92}). The olivine grains have variable NiO content that ranges from 0.1 to 0.5 wt. % (**Fig. 9**). The NiO content was lowest for olivine grains in the Talur mines (0.1-0.2 wt.%). The NiO values were high in dunite of Doddakanya Mines (0.4-0.5 wt. %) and slightly lower for interstitial olivine grains in the net-textured chromitite from the Sindhuvalli mines (0.3-0.4 wt. %). The Fo contents of olivine show a positive relationship with NiO contents (**Fig. 9**).

Chromite - Chromites in massive chromitites are characterized by high *Cr*-number [Cr/(Cr + Al), molar ratio] and high *Mg*-number [(Mg/(Mg + Fe^{2+}), molar ratio)] for the Sindhuvalli mines (**Fig. 10 a**). The *Cr*-number is in the range of 0.67-0.79 and the *Mg*-number is 0.63-0.69. The net-textured chromitite from Sindhuvalli shows wider variations in Cr-number (0.69-0.78) and Mg-number (0.29-0.51). For the massive chromitites from Talur mines, the *Cr*-number is 0.72-0.81 and Mg-number is 0.28-0.39 (**Fig. 10 a**). The schlieren banded chromitites of the Talur mines show restricted variation in both *Cr*-number (0.72-0.74) and *Mg*-number (0.45-0.50). The accessory chromites in dunite from Talur is characterized by low *Mg*-number (0.1-0.12) and high *Cr*-number (0.95-0.98) indicating extensive subsolidus re-equilibration (**Fig. 10 b, c**). The accessory chromites in dunite from Doddakanya mines have a variable *Mg*-number (0.28-0.48) and the *Cr*-number range is 0.73-0.78 (**Fig. 10 b, c**). The high Cr-number in the accessory chromites in dunite is attributed to Al loss during subsolidus re-equilibration.

In the Cr–Al–Fe^{3+} ternary diagram, three distinct compositional characters are recognized for the studied chromite; (1) chemcal variation along the Cr–Al side by the modified chromites in the silicate-rich chromitites (e.g., schelieren banded and net-textured chromitites), (2) chemical variation along the Cr–Fe^{3+} side by the accessory chromites from

the dunite and (3) restricted chemical variation in the unaltered chromites from the massive chromitites of Talur and Sindhuvalli regions (**Fig. 10 e**).

The accessory chromites in dunite from Talur have relatively higher concentration of minor elements like TiO_2, MnO and V_2O_3 than the chromites from chromitites (**Fig. 10 g, h**). TiO_2 and MnO show negative relations with *Mg*-number but both show variable relations with respect to Fe^{3+}- number [Fe^{3+}/(Cr + Al +$Fe3^{+}$) cation ratio]. Accessory chromites in dunite from Doddakanya also show relatively higher concentration of TiO_2 and MnO with higher Fe^{3+}-number (**Fig. 10 d**). In Talur TiO_2 content is 0.9-1.6 wt. %, MnO content is 0.4-0.6 wt. % and Fe^{3+}-number is 0.40-0.44. In Doddakanya TiO_2 content is 0.13-0.31 wt. %, MnO content is 0.1-0.3 wt. % and Fe^{3+}-number is 0.08-0.17. The chromites in massive chromitites from Talur and Sindhuvalli show restricted variations in compositions (**Fig. 10 a**). The chromites in massive chromitites from Talur have TiO_2 of 0.27-0.39 wt. %, MnO of 0.23-0.49 wt. % and Fe^{3+}-ratio of 0.34-0.38. The chromites in Sindhuvalli massive chromitites have TiO_2 of 0.12-0.22 wt. %., MnO of 0.21-0.44 wt. % and Fe^{3+}-number 0.08-0.16. The chromites in massive chromitites of both the areas show lower values of minor elements for constant *Mg*-number, and restricted variation in Fe^{3+}-numbers (**Fig. 10 d**). V_2O_3 shows a variable range over constant *Mg*-numbers, and NiO shows negligible variations in all chromites. The compositional trends of the oxides of the minor elements, with respect to *Mg*-number, are comparable with the trends of the metamorphosed accessory chromites in the Archean komatiitic rocks from Kambalda and Windarra of Australia, as described by Barnes (2000). In these settings, increasing values of TiO_2 and MnO are observed with decreasing Mg-ratios and with increasing grades of metamorphism from greenschist to amphibolite facies.

Chromites from massive chromitites that are genetically linked to komatiitic magma, such as from the Selukwe Railway Block, Zimbabwe, has TiO_2 contents ranging between 0.16 and

0.23 wt. % (Mondal et al., 2006). In contrast, the chromites from the layered intrusions such as the G-chromitite of the Stillwater Complex, Montana, USA, and the UG2 chromitite of the Bushveld Complex, South Africa, have higher TiO_2 contents that range between 0.55–0.67 wt. % and 0.47– 0.98 wt. %, respectively (Mathez and Mey 2005; Mondal et al., 2006). The TiO_2 contents of chromites from the massive chromitites of Sindhuvalli are similar to the komatiitic chromites from the massive chromitites of the Archean Selukwe Railway Block; however, the accessory chromites from dunite have significant higher concentration of TiO_2, in particular in the chromites from the Talur area (**Fig. 10 g**).

8. Discussion

8.1. Compositional variability of chromites and associated silicate minerals

The primary olivine compositions from the Archean greenstone belts are generally in the range of Fo_{91-95}, such as in dunites which are genetically linked to high-Mg komatiitic or boninitic magmas (Rollinson 1997; Barnes 2006; Mondal et al. 2006). The Fo values of olivine in net-textured chromitite in Sindhuvalli (Fo_{95}) are more comparable to the interstitial and included olivine ($Fo_{96–98}$) within chromites from the spotted and massive chromitites of the Archean Nuasahi and Sukinda Massifs in the Singhbhum Craton, India (Mondal et al., 2006). The refractory Fo compositions of olivine in Sindhuvalli net-textured chromitites are due to sub-solidus re-equilibration with the associated chromites. The chromite grains in chromitites, do not show much change in their composition as they represent a modally dominant phase (e.g., Irvine, 1967). The higher values of Fo (in the range of Fo_x-Fo_x) in the next-textured chromitites from the Sindhuvalli region might be due a greater Fe-Mg exchange among chromite and olivine grains in contact with each other. In contrast olivine compositions in dunites from Talur and Doddakanya mines are representing

primary compositions because of minimum possibility of Fe-Mg exchange with the neighboring accessory chromites (e.g., Mondal et al., 2006).

In NiO vs. Fo content plot, we see that the olivines from net-textured chromitite in Sindhuvalli shows much higher Fo content compared to that of olivines from dunites in Doddakanya and Talur. This might be due to sub-solidus re-equilibration of parent melt associated with Sindhuvalli. We also see that the Fo content of the primary olivines in Talur dunite showed lower values compared to that of olivines in Doddakanya dunite. This indicates that the parent melt of Talur was more fractionated compared to Doddakanya.

In Cr# vs. Mg# plot, we see that the chromite compositions from massive chromitite in Talur show lower Mg# compared to that of chromite compositions from Sindhuvalli massive chromitite. This indicates that the parent melt in Talur was also more fractionated compared to Sindhuvalli. The chromites from net-textured chromitite in Sindhuvalli and schlieren banded chromitite in Talur shows almost similar compositions in Cr#-Mg# plot. The accessory chromites in Talur dunite shows high Cr# and low Mg# compared to that of chromites in Doddakanya dunite. The accessory chromite in Talur dunite also has high concentrations of Fe^{3+} as evident in Fe^{3+}-number vs. Mg# plot and Fe^{3+}-Cr-Al ternary diagram. We also observe that each of my samples show distinct Mg# which has a decreasing trend which might indicate possible fractionation of the melt. Our samples are characterized by similar NiO content as evident from NiO vs. Mg# plot. The accessory chromites in Talur dunite show higher TiO_2 and MnO as evident from Fe^{3+} - number vs. TiO_2 and Fe^{3+} -number vs. MnO plots.

The increase in Fe^{3+}, Cr# and TiO_2 in accessory chromites in Talur dunites might due sub-solidus re-equilibration processes associated alterations and metamorphism. The increase in

MnO in accessory chromites in Talur dunite might be related to CO_2-rich fluid activity that ultimately resulted in the formation of magnesite.

8.2. Olivine-chromite geothermometry

Olivine and spinel coexist in a number of geological environments including Alpine peridotites, layered intrusions, meteorites, metamorphic assemblages and basaltic flows. The equilibrium distribution of Fe^{2+} and Mg between these minerals can be expressed as follows (Roeder et al., 1979):

$$1/2Fe_2SiO_4 + Mg(Cr_\alpha Al_\beta Fe_\gamma^{3+})_2O_4 = 1/2Mg_2SiO_4 + Fe(Cr_\alpha Al_\beta Fe_\gamma^{3+})_2O_4$$

where α, β and γ are the atomic fractions of the respective trivalent cations. This exchange is sensitive to temperature, especially for Cr-rich spinel, and Irvine (1965) first described how it may be used as a geothermometer. One of the objectives of this dissertation research work are to calculate the liquidus temperature at the time of magma emplacement as the distribution of Mg and Fe^{2+} between olivine and spinel is a useful guide to the thermal history of various ultramafic-mafic igneous and metamorphic rocks. Experiments on natural samples show the relative ease with which Fe^{2+} and Mg re-equilibrate at temperatures above 1,200^oC (Roeder et al., 1979). The same concept has been applied in our samples from the olivine-chromite assemblage in the dunites from Talur and Doddakanya and net-textured chromitite in Sindhuvalli. This gives the re-equilibrated temperature of the chromite-olivine bearing ultramafic rocks from the three areas. The calculated temperatures of the three study areas have been tabulated in **Table 2**.

The thermometric calculation reveals that the chromite-olivine pairs in Talur area is re-equilibrated to 477-537°C, in Doddakanya area it is in the range of 673-884°C and in Sindhuvalli area it is in the range of 701-750°C. The low temperature in Talur attests the fact that chromite-olivine pair has re-equilibrated till the magnesite formation event which takes

place at lower temperature (400-550°C; Bjerga et al., 2015). In both Doddakanya and Sindhuvalli, chromite-olivine pair has re-equilibrated to the stability field of amphibolite facies metamorphism. If we consider chromite-olivine pairs from different assemblages where modal dominance of chromite and olivine exists individually, such as chromite from massive chromitite and olivine from dunite, the calculated equilibrated temperature for Talur is ≈740°C and that of Sindhuvalli is ≈ 1,211°C. This supports the fact the that the parental magma in Talur had a more evolved nature compared to Sindhuvalli and Doddakanya and supports the conclusions drawn from the earlier section.

8.3. Calculations of parental melt and implications for tectonic settings

The unaltered and primitive chromite compositions, from the massive chromitites that display limited compositional variability (**Fig. 10 a**), have been used to compute the parental melt compositions in terms of the FeO/MgO ratio, TiO_2 and Al_2O_3 contents. The Al_2O_3 of the liquid is computed from Maurel and Maurel (1982) for spinel-liquid equilibrium at 1 bar where,

$$(Al_2O_3)_{spinel} = 0.035(Al_2O_3)^{2.42}{}_{liquid}$$

This equation is based on the observation that the Al_2O_3 (wt. %) in spinel is a function of Al_2O_3 (wt. %) in melt (e.g., Mondal et al., 2006). Kamenetsky et al. (2001) also showed from the melt inclusion data within chromite from volcanic rocks that there is a linear relationship between the Al_2O_3 and TiO_2 content in chromite, and the Al_2O_3 and TiO_2 content in the melt from which it crystallized. Using the relation of Kamenetsky et al. (2001) from above, the Al_2O_3 content of parental melt for Talur and Sindhuvalli chromitite is obtained. For Sindhuvalli, net-textured chromitite is also used. The values of Al_2O_3 of the parental melt calculated from the above methods are found to correspond closely. The FeO/MgO ratio of the liquid is computed from the primitive chromite composition using the Maurel and

Maurel's (1982) equation, where $\ln(FeO/MgO)_{spinel} = 0.47 - 1.07Y_{spinel}\,Al + 0.64YFe_{spinel}^{3+} + \ln(FeO/MgO)_{liquid}$ where, $Y_{spinel}\,Al = Al/(Cr + Al + Fe^{3+})$ and $Y_{spinel}\,Fe^{3+} = Fe^{3+}/Cr + Al + Fe^{3+})$. The TiO_2 content of the melt is obtained from the melt-TiO_2 versus chromite-TiO_2 diagram of Kamenetsky et al. (2001).

The computed values of Al_2O_3, TiO_2 and FeO/MgO ratio of the melt have been tabulated in **Table 3**. It is observed that the Al_2O_3 content of the melt is more or less similar for the three areas. The Al_2O_3 content of Sindhuvalli is slightly higher (12.03-13.53 wt. %). The TiO_2 concentration of the melt is low and is found in the range of 0.11-0.49 wt. % in Sindhuvalli and 0.14-0.43 wt. % for Talur. On comparing the calculated melt parental melt from this study with primitive magmas from different tectonic settings, our data are found to show closest resemblance with Archean low-Al_2O_3 komatiitic magmas (**Table 4**).

The primary chromite compositions from the Sargur schist belt are compared with the compositions of chromites from the Archean greenstone belts and the Archean layered complexes (**Table 4**). In the tectonic discrimination diagram of Cr-ratio versus Mg-ratio and the Cr-Al-Fe^{3+} ternary diagram, the majority of the primary chromite compositions from Talur and Sindhuvalli plot within the field of chromites from komatiites. This is also supported by the calculations which indicate komatiitic melt was the possible parental magma composition for the studied chromites from the Sargur schist belt.

8.4. Genesis of chromitites

Formation of massive chromitites require the parental magma to be saturated with only chromite, relative to other phases, as this would eventually precipitate a monomineralic layer of chromitite. There are various theories that have been proposed to explain the above phenomenon such as increase in total pressure (Cameron 1977; Lipin 1993), fO_2 (Cameron and Desborough 1969; Ulmer 1969; Murck and Campbell 1986) and $aSiO_2$ through

contamination (Irvine 1975). However, the most acceptable theory is that of magma mixing model proposed by Irvine (1977). All these existing models of chromitite formation have been recently reviewed by Mondal and Mathez (2007). In addition, the chromitite bodies in may be formed as intrusives of chromite crystal slurry (e.g., Mondal and Mathez, 2007). The magma mixing model (Irvine 1977) explained that the mixing of a chemically primitive mafic melt with a more evolved mafic melt can cause the hybrid magma to be supersaturated with chromite alone; thus, a monomineralic chromitite layer would eventually form by subsequent settling. This is due to the curved nature of the olivine–chromite cotectic in the $MgO–Cr_2O_3–SiO_2$ system. The hybrid magma is expected to be less differentiated than the originally evolved magma present in the magma chamber prior to mixing. This would result in variation in the Mg/Fe ratios within the entire sequence; the rocks above the chromitite layer are expected to possess greater Mg/Fe ratios than the ones below it. Furthermore, mixing of two magmas with different fO_2 and temperature is also expected to produce a hybrid magma supersaturated in chromite (e.g., Murck and Campbell 1986). In the Sargur schist belt, the host peridotitic rocks for the massive chromitite are extensively altered to magnesite and serpentine. Therefore, there is little scope to test the magma mixing model for the studied chromitites. However, there are indications of the presence of slightly different melt compositions in different mining areas that may support the mixing model.

9. Conclusions

The main conclusions of this study are: -

1. The compositional variations in chromites show that Talur has relatively fractionated parental melt composition compared to Sindhuvalli and Doddakanya.

2. The olivine-chromite thermometry attests the fact that the olivine-chromite pairs in both Sindhuvalli and Doddakanya have preserved temperatures corresponding to amphibolite facies metamorphism whereas in Talur, the calculated temperature might be related to CO_2-rich fluid activity.
3. The possible parental magma for chromites in Sargur schist belt may be komatiitic in nature which is common in early Archean greenstone belts.

References

Bjerga, A. 2015. Talc-carbonate alteration of ultramafic rocks within the Leka Ophiolite Complex, Central Norway. Lithos 227 (2015) 21–36.

Acharyya, S.K., 1993. Greenstones from Singhbhum Craton, their Archaean character, oceanic crustal affinity and tectonics. Proc. Natl. Acad. Sci. India 63 (A), 211–222.

Allegre, C.J., 1982. Genesis of Archaean komatiites in a wet ultramafic `subducted plate. In: Arndt, N.T., Nisbet, E.G. (Eds.), Komatiites. George Allen and Unwin, pp. 495–500.

Auge, T., 1987. Chromite deposits in the northern Oman ophiolite: ´mineralogical constraints. Miner. Dep. 22, 1–10.

Banerjee, P.K., 1972. Geology and geochemistry of the Sukinda ultramafic field, Cuttack district, Orissa. Memoir Geol. Surv. India 103, 171.

Barley, M.E., 1986. Incompatible element enrichment in Archaean basalts: a consequence of contamination by older sialic crust rather than mantle heterogeneity. Geology 14, 1–15.

Barnes, S.J., 2000. Chromite in Komatiites. II. Modification during greenschist to mid-amphibolite facies metamorphism. J. Petrol. 41, 387–409.

Barnes, S.J., Roeder, P.L., 2001. The range of spinel compositions in terrestrial mafic and ultramafic rocks. J. Petrol. 42, 2279–2302.

Basu, A., Maitra, M., Roy, P.K., 1997. Petrology of mafic-ultramafic complex of Sukinda valley, Orissa. Indian Miner. 50, 271–290.

Droop, G.T.R., 1987. A general equation for estimating Fe^{3+} concentrations in ferromagnesian silicates and oxides from microprobe analysis, using stoichiometric criteria. Miner. Mag. 51, 431–435.

Irvine, T.N., 1967. Chromian spinel as a petrogenetic indicator. Part II. Petrological applications. Can. J. Earth Sci. 4, 71–103.

Irvine, T.N., 1975. Crystallization sequences in the Muskox intrusion and other layered intrusions-II. Origin of chromitite layers and similar deposits of other magmatic ores. Geochim. Cosmochim. Act a 39, 991–1020.

Irvine, T.N., 1977. Origin of chromitite layers in the Muscox intrusion and other stratiform intrusions: a new interpretation. Geology 5, 273–277.

Kamenetsky, V.S., Crawford, A.J., Meffre, S., 2001. Factors controlling chemistry of magmatic spinel: an empirical study of associated olivine, Cr-spinel and melt inclusions from primitive rocks. J. Petrol. 42, 655–671.

Mathez E.A., Mey, J.L., 2005. Character of the UG2 chromitite and host rocks and petrogenesis of its pegmatoidal footwall, northeastern Bushveld complex. Econ Geol 100:1617–1630.

Mondal, S.K., Ripley, EM, Li C, Frei R (2006) The genesis of Archean chromitites from the Nuasahi and Sukinda massifs in the Singhbhum craton, India. Precambrian Res 148:45–66.

Mukherjee, R., Mondal, S.K., Rosing, M.T., Frei, R., 2010. Compositional variations in the Mesoarchean chromites of the Nuggihalli schist belt, Western Dharwar Craton (India): potential parental melts and implication for tectonic setting. Contrib. Mineral. Petrol. 160, 865–885.

Maurel, C., Maurel, P., 1982. Etude experimentale de la solubilit ´ e du ´ chrome dans les bains silicates basiques et sa distribution entre ´ liquide et mineraux coexistants: conditions d'existence du spinelle ´ chromifere. Bulletin Min ´ eralogie 105, 197–202.

Roeder, P.L., 1994. Chromite: from the fiery rain of chondrules to the Kilauea Iki lava lake. Can. Mineral. 32, 729–746.

Roeder, P.L., Emslie, R.F., 1970. Olivine-liquid equilibria. Contrib. Mineral. Petrol. 29, 275–289.

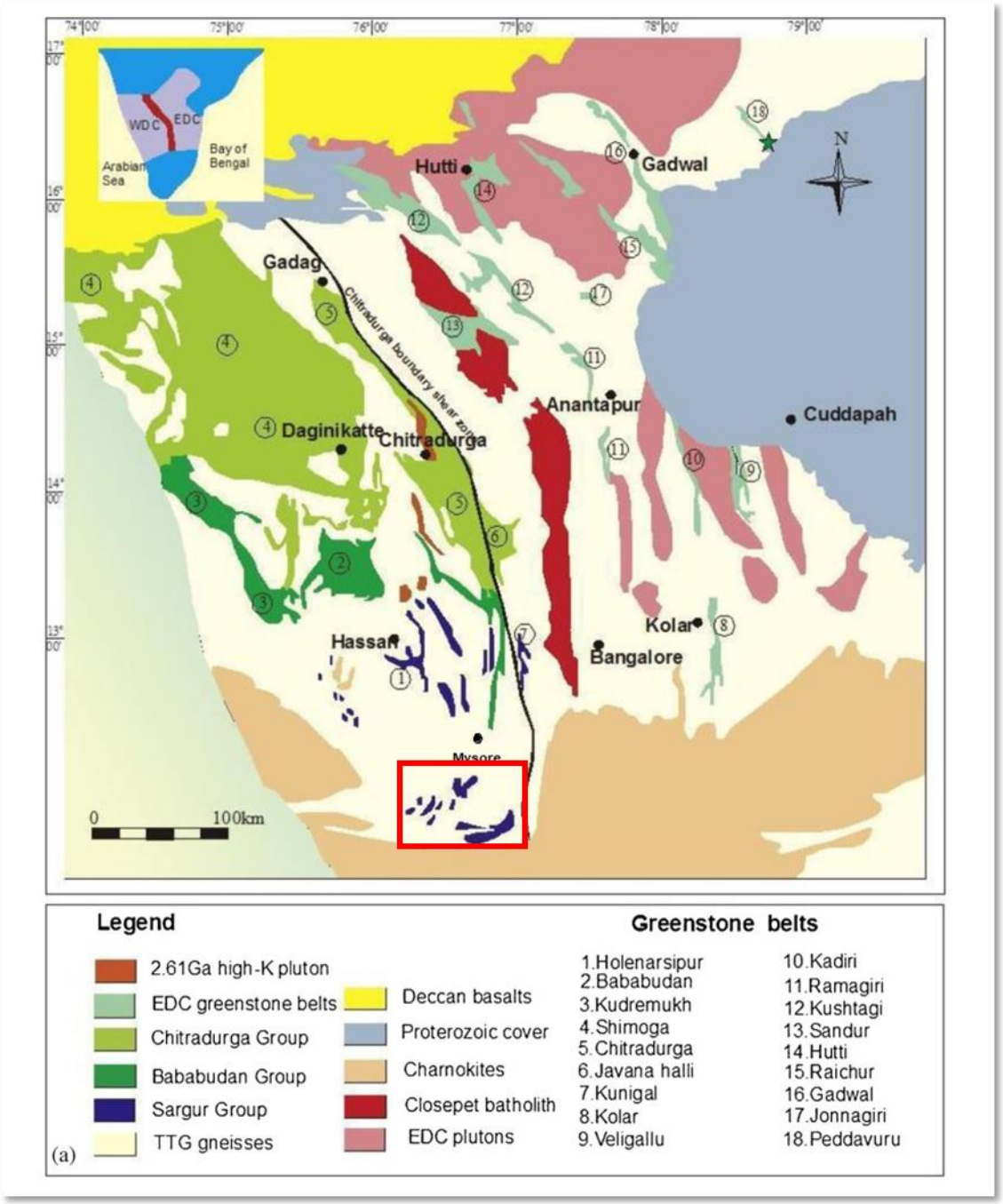

Fig 1 – Geological map of the Dharwar Craton (Rajamanickam et al., 2014).

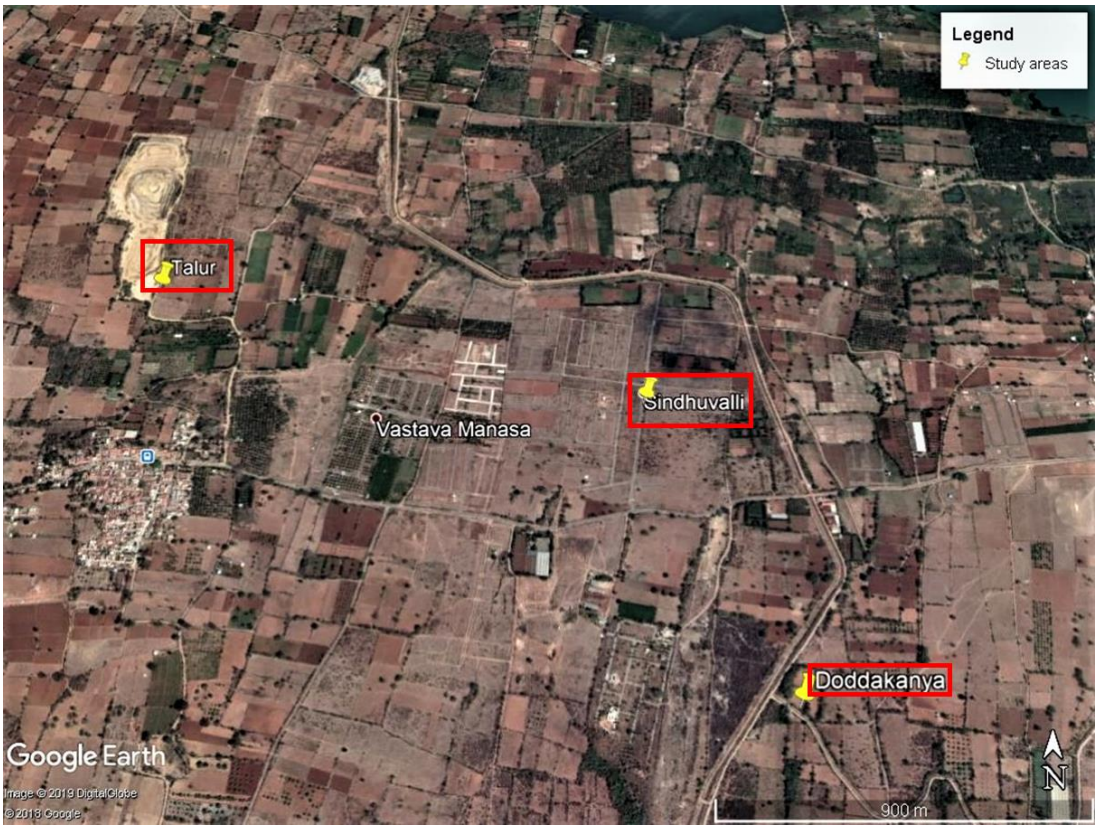

Fig 2: - Locations of the chromite mining districts. Sample locations are marked.

Fig 3 – Photographs of hand specimens illustrating different textures in chromite bearing rocks from Talur Magnesite Mines. **a.** Dunite. **b.** Massive chromitite. **c.** Schlieren banded chromitite. **d.** Net-textured chromitite.

Fig 4: - Photographs of hand specimens illustrating different textures in chromite bearing rocks from Sindhuvalli Mines. **a.** Net-textured chromitite. **b.** Massive chromitite.

Fig 5: - Photographs of hand specimens showing accessory chromite grains in dunite rocks collected from Doddakanya.

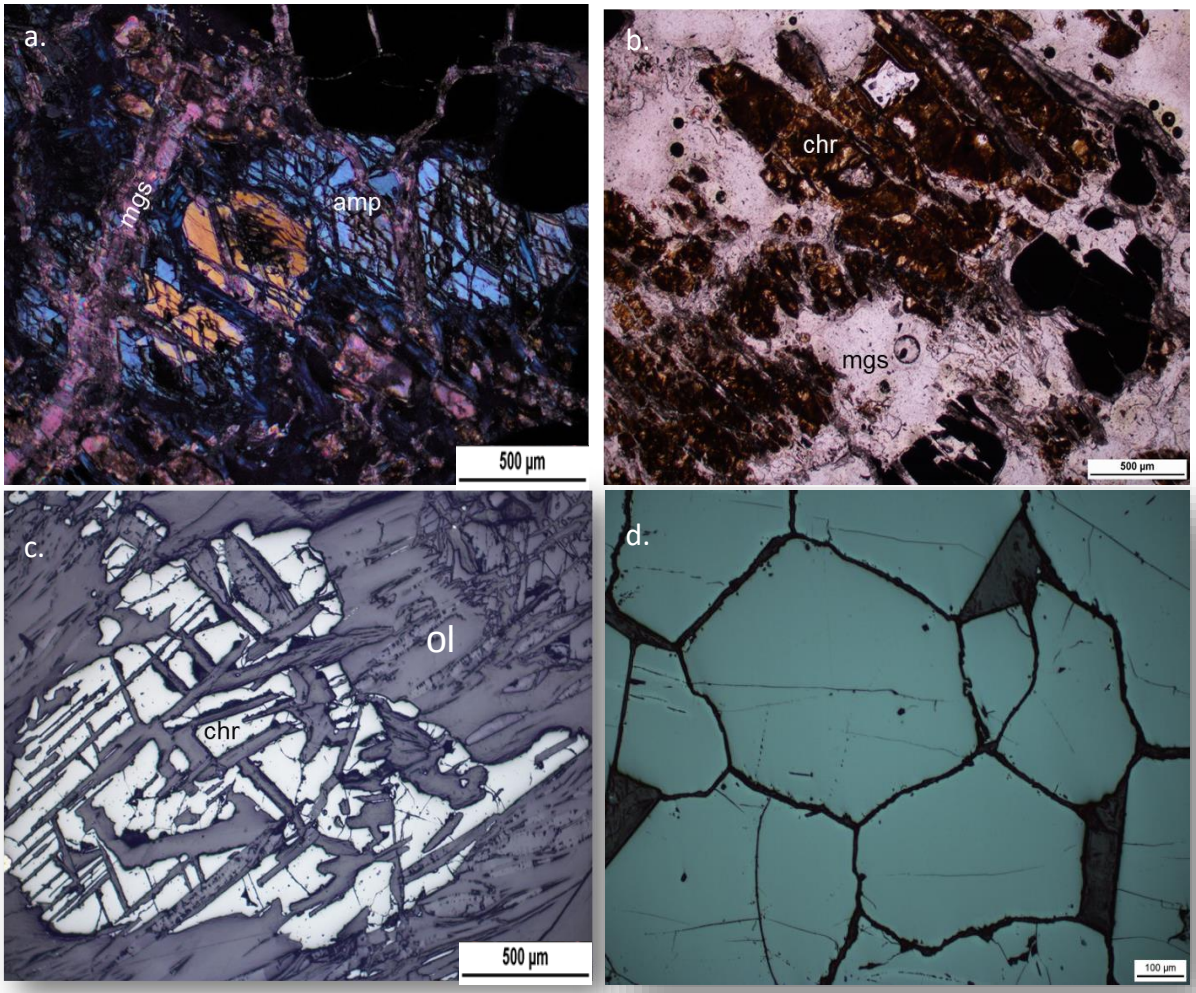

Fig 6: - Photomicrographs of the samples from Talur magnesite mines. **a.** Optical image of tremolite in association with chromite grains and serpentine. Magnesite micro-vein transgresses through the entire assemblage. **b.** Optical image showing highly altered chromite grains in association with magnesite in net-textured chromitie. **c.** Optical image of oxidised and deformed accessory chromite grain in dunite. **d.** Optical image showing chromite grains showing polygonal shape in massive chromitite characterized by very low interstitial minerals.

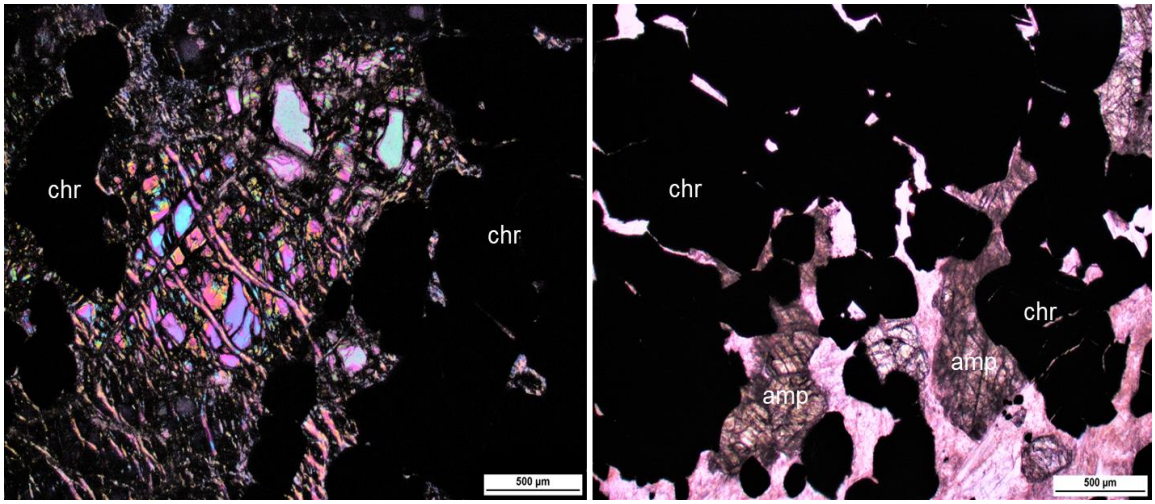

Fig 7: - Photomicrographs of samples collected from Sindhuvalli mines.
a. Optical image of net-textured chromitite showing highly altered olivine in association with subhedral chromite grains. **b.** Optical image of massive chromitite showing large subhedral to anhedral chromite grains getting replaced by tremolite.

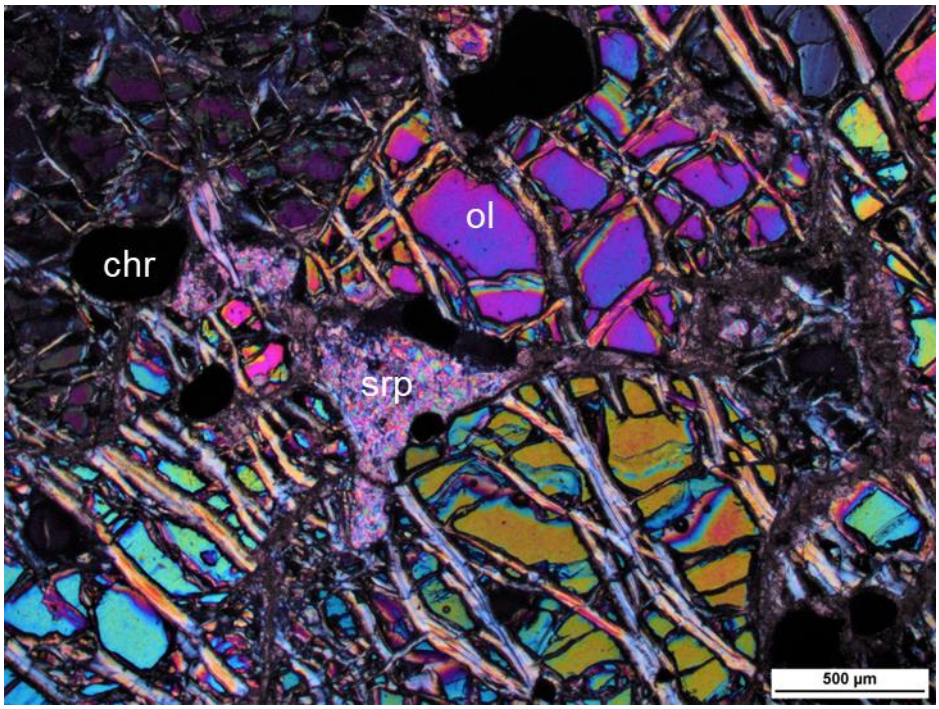

Fig 8: - Photomicrograph of a dunite sample collected from Doddakanya. The olivine grains are highly altered by serpentine. Accessory opaque chromite grains are observed in the assemblage.

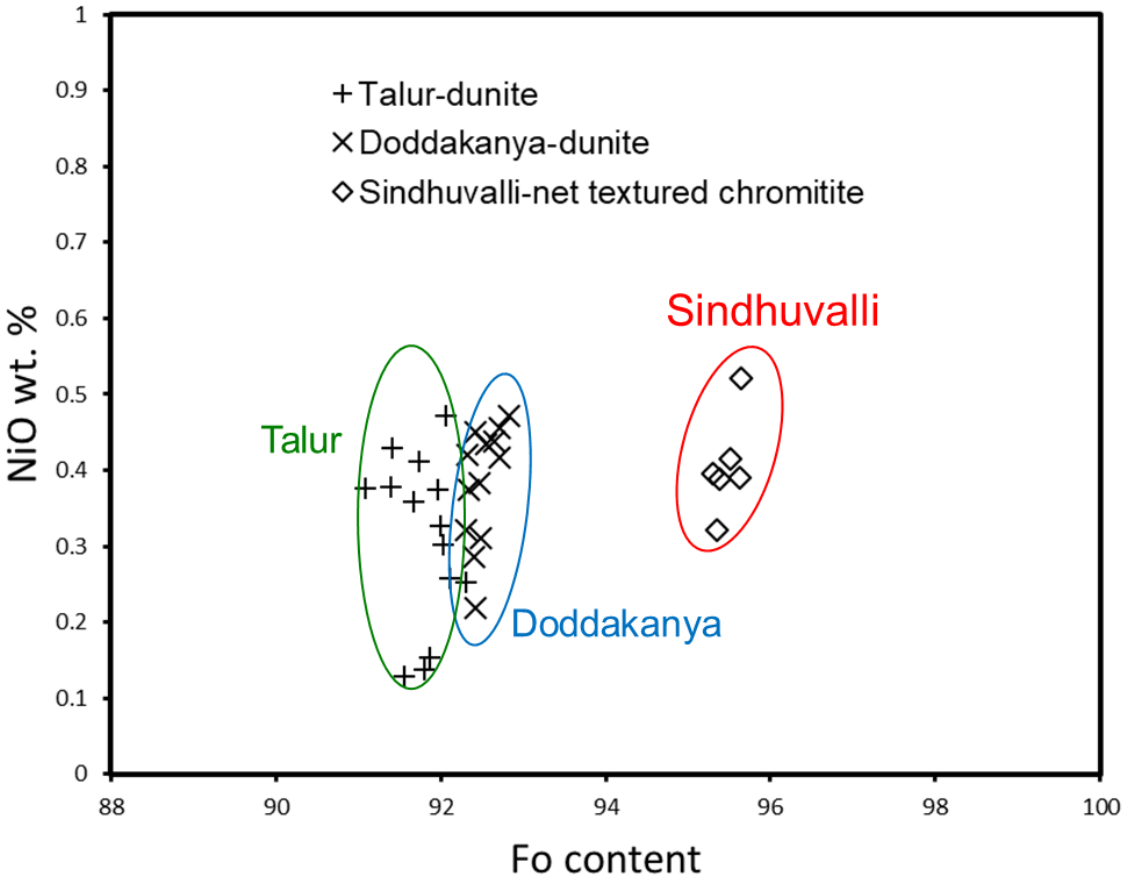

Fig 9: - Variation diagrams for composition of olivine from Talur dunite, Sindhuvalli net-textured chromitite and Doddakanya dunite – NiO-Fo content diagram in olivine.

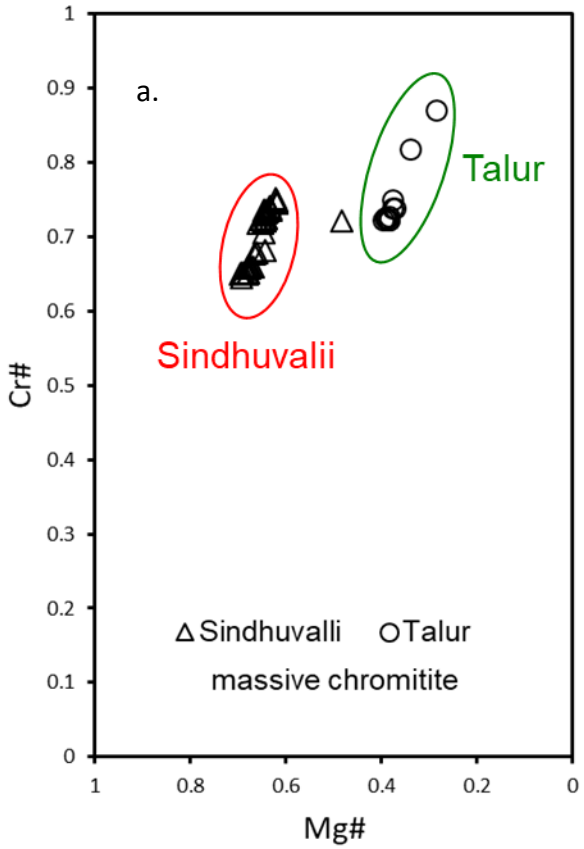
a.
Talur
Sindhuvalii
Cr#
Mg#
Sindhuvalli
Talur
massive chromitite

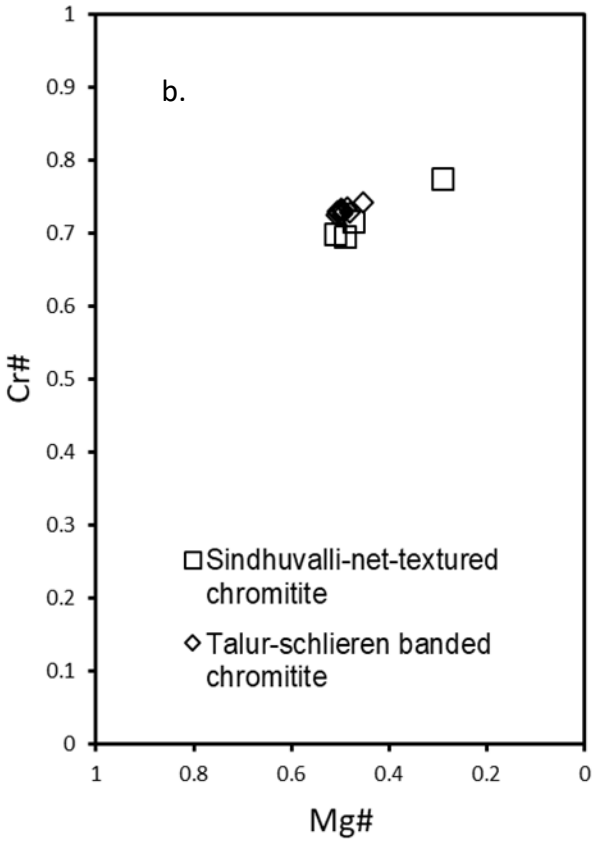
b.
Cr#
Mg#
Sindhuvalli-net-textured chromitite
Talur-schlieren banded chromitite

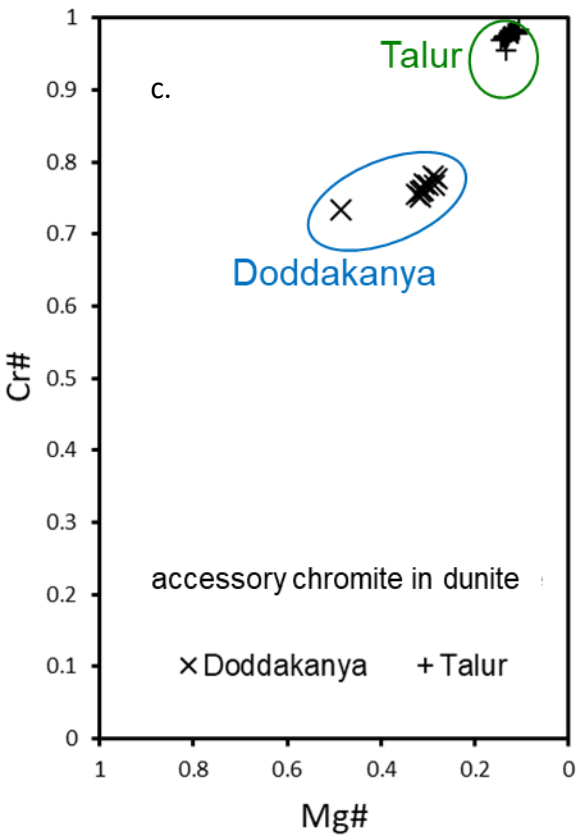
c.
Talur
Doddakanya
Cr#
Mg#
accessory chromite in dunite
Doddakanya
Talur

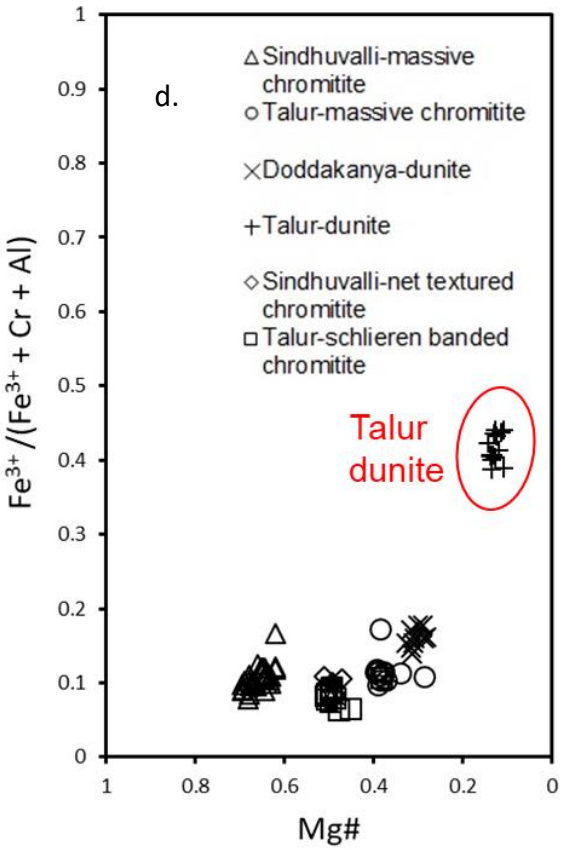
d.
Sindhuvalli-massive chromitite
Talur-massive chromitite
Doddakanya-dunite
Talur-dunite
Sindhuvalli-net textured chromitite
Talur-schlieren banded chromitite
Talur dunite
Fe3+/(Fe3+ + Cr + Al)
Mg#

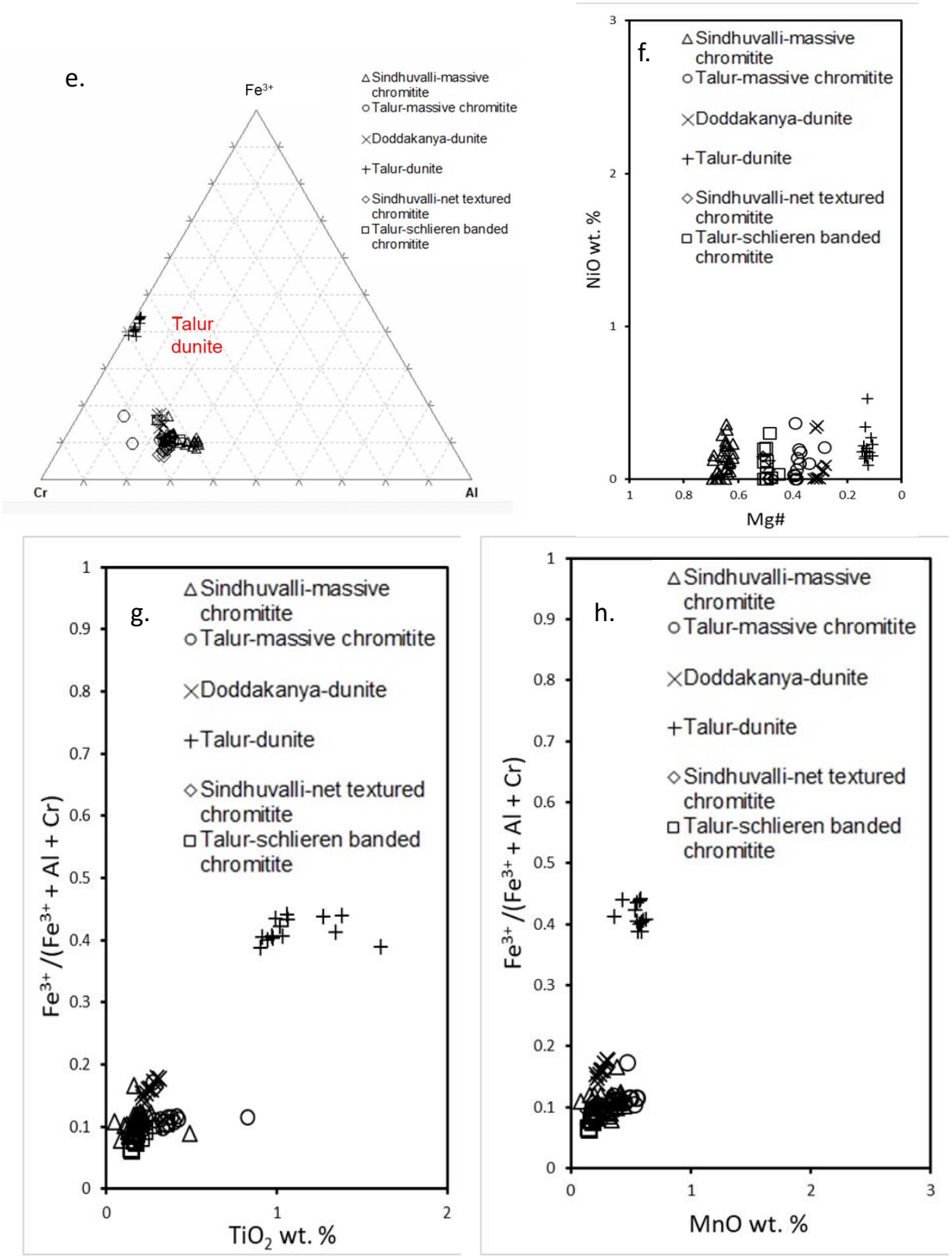

Fig 10: - Variation diagrams for composition of chromites from Talur, Sindhuvalli and Doddakanya areas. **a.** Cr#-Mg# variation seen in chromites from massive chromitites. **b.** Cr#-Mg# variation seen in net-textured chromitite and schlieren banded chromitite. **c.** Cr#-Mg# variation seen in accessory chromites in dunite. **d.** Trivalent cation ratios vs Mg# variation from chromites of the present study. **e.** Fe^{3+}-Cr-Al ternary plot. **f.** Variation of NiO plotted against the Mg-ratio for chromites of the study areas. **g, h.** Variation of $Fe^{3+}/Cr + Al + Fe^{3+}$ ratio plotted against TiO_2 and MnO for chromites in our study area.

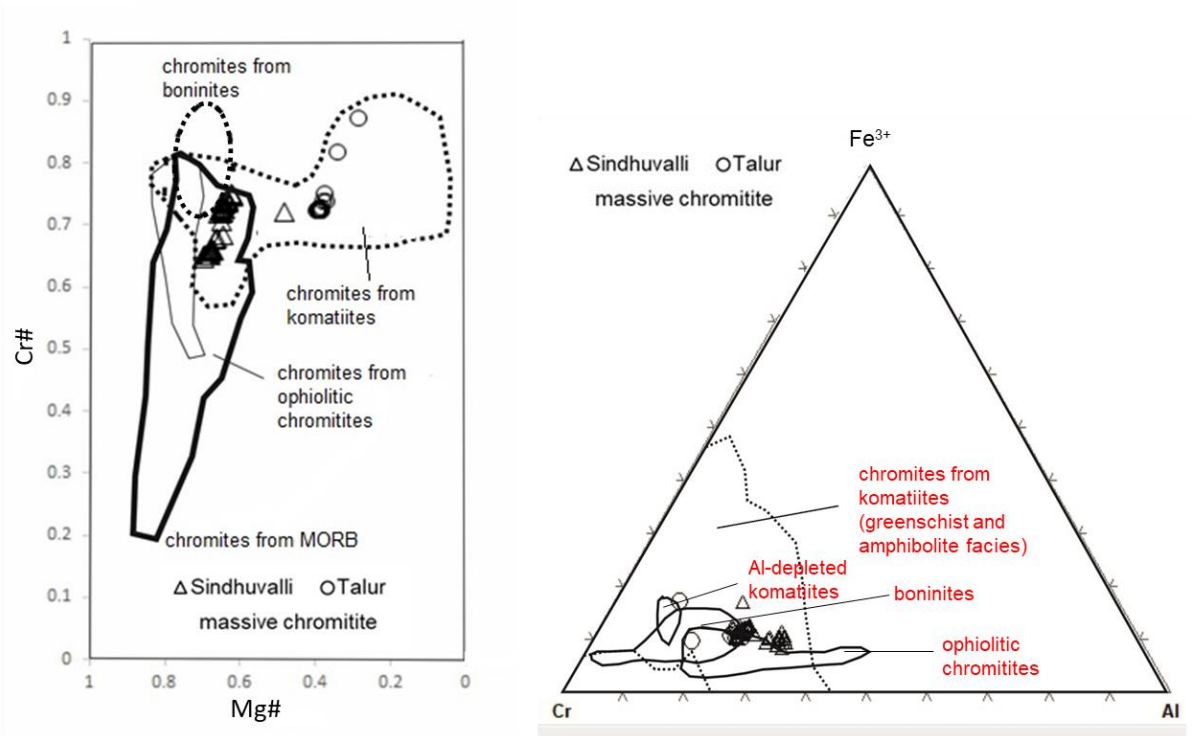

Fig 11: - Possible parental magmas. **a.** Cr#–Mg# variations in chromites compared with primitive magma (fields are after Barnes and Roeder, 2001); **b.** trivalent cation plot of chromites from massive chromitite in comparison with chromites associated with boninites, ophiolites and komatiites (fields are after Barnes and Roeder, 2001).

TABLE 1: -

List of studied samples with modal abundances.

Sample no.	Location	Rock type	Mineralogy	Modal
DHR-12-01	Talur	Schlieren banded chromitite	chr+ol+srp+mgs+tlc	chr-40%, ol-25%, srp-25%, mgs-5%, tlc-5%
DHR-12-02	Talur	Net-textured chromitite	chr+srp+mgs	chr-75%, srp-20%, mgs-5%
DHR-12-03	Sindhuvalli	Net-textured chromitite	chr+ol+srp+pyx+amp+mgs	chr-45%, ol-25%, srp-15%, pyx-10%, amp-5%, mgs-5%
DHR-12-05	Doddakanya	Dunite	ol+srp+chr+pyx+mgs	ol-40%, srp-20%, chr-15%, pyx-15%, mgs-10%
DHR-12-06	Doddakanya	Dunite	ol+srp+chr+mgs	ol-40%, srp-35%, chr-20%, mgs-5%

DHR-12-07	Doddakanya	Dunite	ol+srp+chr+mgs	ol-45%, srp-30%, chr-20%, mgs-5%
DHR-12-08	Doddakanya	Dunite	ol+srp+chr	ol-60%, srp-30%, chr-10%
DHR-12-09	Doddakanya	Dunite	ol+srp+cr+mgs	ol-50%, srp-25%, chr-15%, mgs-10%
DHR-13-74	Talur	Schlieren banded chromitite	chr+srp+amp+mgs	chr-50%, srp-25%, amp-20%, mgs-10%
DHR-13-75	Talur	Dunite	srp+ol+chr+mgs	ol-50%, srp-25%, chr-15%, mgs-10%
DHR-13-76	Talur	Chromitite	chr+ol	chr-95%, ol-5%
DHR-13-77	Sindhuvalli	Chromitite	chr+ol+mg+srp	chr-85%, ol-5%, mgs-5%, srp-5%

Table 2: -

Calculated temperatures for re-equilibrated chromite-olivine pairs in my study areas

Location	Rock type	Temperature range (ºC)
Talur	dunite	477-537
Doddakanya	dunite	674-884
Sindhuvalli	net-textured chromitite	708-750

Table 3: -

Al_2O_3 content, FeO/MgO ratio and TiO_2 content in the parent melt of chromites in Sargur greenstone belt, WDC.

Sargur schist belt, WDC	Al_2O_3 liquid wt. %	FeO/MgO liquid	TiO_2 liquid wt. %
Talur – massive chromitite	8.6-12.7	2.04-2.79	0.23-0.43
Talur – schlieren banded chromitite	12.43-13.11	1.33-2.16	0.14-0.35
Sindhuvalli – massive chromitite	10.66-13.05	0.64-1.46	0.11-0.49
Sindhuvalli net-textured chromitite	11.22-13.53	1.32-2.99	0.18-0.29
Nuggihalli greenstone belt, WDC	8.38-10.63	0.94-1.49	0.46-0.92

Table 4: -

Computed parental melt of the Sargur chromitite calculated from primary chromite compositions and comparison with other ultramafic–mafic magmas

	Al_2O_3 liquid (wt.%)	FeO/MgO liquid	TiO_2 (wt. %) liquid
Sargur schist belt, WDC	8.6-13.11	0.45-2.79	0.11-0.49
Nuggihalli greenstone belt, WDC	8.38-10.63	0.94-1.49	0.23-0.43
IOG high-Mg basalts			
Nuasahi area	7.9	0.52	
Sukinda area	10.7	0.94	
Gorumahishani-Badampahar (Eastern) Belt	8.8	0.91	
Selukwe chromitite (Railway Block)	11.8–12.2	0.54–0.60	
Stillwater G chromitite	12.3–12.6	1.48–1.58	
Ophiolitic chromite deposits			
Oman chromitite	11.4–16.4	0.62 ± 0.02	
Layered Intrusions (parental magma)			
Bushveld (Average 'U' Type)	11.5	0.74	
Great Dyke	11.1	0.61	
Archaean low-Ti siliceous high-Mg basalts			
Barberton	12.7–13.4	0.74	0.31-0.33
Pilbarah	10.1–11.7	0.58–0.75	0.39-0.43
Boninites	10.6–14.4	0.7–1.4	
MORB	~15	1.2–1.6	
Komatiitic basalts, Archean greenstone belts			
Tisdale township, Abitibi greenstone belt	8.58–9.38	0.74–0.85	0.53–0.57
J.C. Pura belt, Western Dharwar Craton	8.91	0.66	0.46
Kalyadi belt, Western Dharwar Craton	7.9	0.66	0.4

Mondal et al. (2006); Mukherjee et al. (2010)